Regular Article

PHYSICAL CHEMISTRY RESEARCH
Published by the
Iranian Chemical Society
www.physchemres.org
info@physchemres.org

Phys. Chem. Res., Vol. 14, No. 2, 239-249, June 2026
DOI: 10.22036/pcr.2026.556005.2773

Exploring the Structural and Functional Competence of Spinal Ferrites (AB_2O_4) for Sensing and Photocatalytic Applications

S. Swamy[a], D.B. Aruna Kumar[a,*], K. Gurushantha[b,*], S. Shashidhar[c,*], S. Meena[d,*], K.V. Brungesh[e], T. Ramakrishnappa[f] and K.M. Girish[g]

[a]*Department of Studies and Research in Chemistry, University College of Science, Tumkur University, Tumkur-572103, India*
[b]*Department of Chemistry, M.S. Ramaiah Institute of Technology (Affiliated to Visvesvaraya Technological University, Belgaum), Bengaluru-560054, India*
[c]*Department of Chemistry, New Horizon College of Engineering, Bengaluru-560103, Karnataka, India*
[d]*Department of Chemistry, Dayananda Sagar College of Engineering, Bengaluru-560111, India*
[e]*Department of Chemistry, Acharya Institute of Technology, Bengaluru-560107, India*
[f]*Department of Chemistry, BMS Institute of Technology and Management, Yelahanka, Bengaluru-560019 Karnataka, India*
[g]*Department of Physics, Dayananda Sagar Academy of Technology and Management, Bangalore 560082, India*
(Received 29 October 2025, Accepted 1 February 2026)

In this study, spinel ferrite nanoparticles $CoFe_2O_4$, $NiFe_2O_4$, $CuFe_2O_4$ and $ZnFe_2O_4$ were synthesized via the solution combustion method and evaluated for the photocatalytic degradation of Allura Red, a persistent azo dye commonly found in industrial wastewater. The rapid combustion process yielded porous, nanostructured ferrites with high surface area, as confirmed by SEM analysis. Structural and elemental integrity was verified using XRD and EDS techniques. Among the synthesized catalysts, variations in morphology and surface characteristics significantly influenced their degradation efficiency of Allura Red dye under visible light irradiation. The $CuFe_2O_4$ has been the 91.3% which is the least and the $ZnFe_2O_4$ shows the highest at 97.5% degradation. The results highlight the potential of transition metal ferrites as cost-effective and efficient photocatalysts for environmental remediation. Further synthesized ferrites were showing the best results in sensing dopamine, hence these results show multiple application of the ferrites.

Keywords: Spinal ferrites, Photocatalytic degradation, Sensor, Dopamine

INTRODUCTION

Dumping of synthetic dyes in the water forms a very urgent environmental issue as they remain persistent, partly very toxic compounds, as well as possible carcinogens, especially when they accumulate as a result of the textile, food, leather, and cosmetic industries. Among them, the common food dye Allura Red (ARD), which is highly soluble and comprises a difficult structure with sensitive aromaticity, has been challenged to biodegrade [1]. It is widely applied in food and drinks, but its discharge to water systems, even in tiny amounts, has carcinogenic, mutagenic and cytotoxic properties. The degradation of such recalcitrant dyes has traditionally been very difficult to remove using conventional wastewater treatment processes, and hence the need to come up with new, effective wastewater treatment techniques that are also environmentally friendly [2].

Complex dyes like Allura Red are not always totally degraded by the traditional processes like adsorption or coagulation. Conversely, advanced oxidation processes (AOP) such as heterogeneous photocatalysis have come up as potential means to mineralize persistent organic pollutants

*Corresponding authors. E-mail: gurushanthak2016@gmail.com; meena23286@gmail.com; shashidharchem32@gmail.com; arunkumar@tumkuruniversity.in

into non-toxic by-products (CO_2 and H_2O) under visible or UV light. The significant aspect of this approach is the capacity of the photocatalyst to produce reactive oxygen species (ROS) and have a charge separation. The selection of a photocatalyst is the main element of AOPs [3-5].

Such noted transition metal ferrites are MFe_2O_4 with the general formula M = Co, Cu, Ni, Zn, which have been utilized in recent years due to having a high value of magnetic, electronic and optical properties. A set of ferrites, MFe_2O_4 (M = Co, Cu, Ni, Zn), has become promising photocatalysts because: their semiconducting character with narrow band gaps, making them absorb visible light, outstanding thermal stability, chemical stability and recovery of their magnetic character in a simple manner [6-8]. Structural, morphological, and electronic properties can be refined by the substitution of various transition metal ions at the divalent M-site and impact on the charge separation, surface adsorption, and the production of reactive oxygen species (ROS) in the course of photocatalysis [9,10].

Here are a couple of tips from the reported studies on the ferrites MFe_2O_4 (where M = Co, Cu, Ni, Zn) [11]. Singh & Soni *et al.* proved $CoFe_2O_4$ to be exhibiting powerful magnetism and chemical resistance [12]. $CuFe_2O_4$ was synthesized [13] through the combustion technique, and it shows higher conductivity along with a narrow band gap, which is optimal as an ROS generator. Pan *et al.* gave $NiFe_2O_4$ witch has good charge mobility and is used extensively in visible-light catalysis.[14] The degradation of Allura Red dye by $ZnFe_2O_4/TiO_2$ where $ZnFe_2O_4$ is the important ingredient which is functional at the visible wavelengths and develops efficient heterojunctions, was published by Al-Hetlani & Al-Kandari [15].

The solution combustion method (SCM) is commonly used in synthesizing such nanostructured ferrites with requisite morphology and higher surface area. SCM is an energy and cost-efficient alternative synthetic method, as fast, cost-effective and energy efficient since it is founded on an exothermic redox reaction that is self-sufficient. The advantages of this method include a low temperature of synthesis, reduced reaction time, molecular level mixing that results in highly crystalline and high porosity with large surface areas during the final product, witch is favorable to catalytic purposes [16].

We have described here the synthesis of $CoFe_2O_4$, $NiFe_2O_4$, $CuFe_2O_4$ and $ZnFe_2O_4$ nanoparticles through the solution combustion method and their utilization in the degradation of Allura Red dye under visible light illumination. Techniques employed to characterize the structural, morphological, optical and magnetic properties of the synthesized ferrites thoroughly XRD, SEM, HRTEM and UV-Vis spectroscopy. The photocatalytic activity was measured in terms of the degradation rate of Allura Red dye in the aqueous solution systematically studied. The objective of the work is to comparatively illuminate the photocatalytic activity of various transition metal ferrites and correlate the physicochemical properties of various ferrites to the dye degradation activity, thus leading the way to the formulation of effective materials in the treatment of wastes and environmental rehabilitation. The detection of dopamine, along with photocatalytic degradation studies for the transition ferrites, shows the novelty of the work.

EXPERIMENTAL

Materials

Cobalt nitrate hexahydrate [$Co(NO_3)_2.6H_2O$], nickel nitrate tetrahydrate [$Ni(NO_3)_2.6H_2O$], copper nitrate [$Cu(NO_3)_2$], zinc nitrate [$Zn(NO_3)_2.6H_2O$], iron nitrate nonahydrate [$Fe(NO_3)_2.9H_2O$],urea [CH_4N_2O] and AR dye, all of analytical grade reagents were procured from lobo chemicals ltd, all these chemical were used as such.

Synthesis

For the synthesis of cobalt ferrite, a 1:2 ratio of cobalt nitrate hexahydrate and iron nitrate nanohydrate, along with urea, which acts as an oxidizer (fuel) was taken in petri dish. Add 50 ml of distilled water to dissolve and make homogeneous solution by using a magnetic stirrer for 20 min at 60 °C to get a viscous solution. The redox mixture is kept in a muffle furnace, which is preheated at 450 ± 50 °C. The mixture started to boils, then dehydration occured. The solution starts decomposes, resulting in the formation of cobalt ferrites with a large amount of gases liberated. The entire process was completed within 10 min. The obtained cobalt ferrite was calcinated at 600 °C for 3 h. Similarly, nickel, copper, and zinc ferrites were prepared.

The resulting ferrites were characterized employing Bruker PXRD. The morphological analysis and size of the particle were known by scanning electron microscopy (SEM) and Transmission electron microscopy (TEM). The UV-Visible reflectance spectra were verified on PerkinElmer UV-Visible Lambda 365 spectrophotometer. An electrochemical analyser CHI608E potentiostat with a tri-electrode system was used to measure Cyclic Voltammetry (CV), EIS and sensor measurements, which include a combined graphite powder electrode, platinum wire and Ag/AgCl as working, counter and reference electrodes, respectively and 1.0 M KCl solution as the electrolyte.

Photocatalytic Studies

Using a circular glass reactor and a 125 W medium-pressure mercury vapor lamp as the light source, the photocatalytic tests were conducted at room temperature. Light was directly focused into the reaction mixture in the open air at a distance of 25 cm in order to carry out the irradiation. Double-distilled water was used for every experiment. In a standard experiment, 250 ml of a 10 ppm allura red dye solution was mixed with 50 mg of photocatalyst metal ferrites (MFe_2O_4). For the duration of the experiment, a magnetic stirrer was used to vigorously swirl the reaction mixture. To guarantee the establishment of adsorption/desorption equilibrium, the reaction mixture was agitated for 30 min prior to irradiation. The equation $Q = (C_0 - C)\ V/W$ was used to determine the extent of adsorption, where "Q" stands for the extent of adsorption, C_0 and C for the concentrations before and after degradation, V for the reaction mixture's volume, and W for the amount of catalyst present in mg. The residual content of allura red dye was ascertained by centrifuging the reaction mixture at predetermined intervals and subjecting it to spectrophotometric measurement.

RESULTS AND DISCUSSIONS

X-ray Diffraction (XRD) Analysis

X-ray diffraction (XRD) was perceptible in the crystalline phases of the synthesized $CoFe_2O_4$, $CuFe_2O_4$, $NiFe_2O_4$, and $ZnFe_2O_4$ nanoparticles. According to the standard JCPDS files, the diffraction patterns (2θ range: 20° to 80°) indicated that all the samples formed a single-phase spinel ferrite structure, which met the jack of $CoFe_2O_4$ (JCPDS No. 22-1086). For $CuFe_2O_4$ (JCPDS No. 34-0425) along with trace amounts of CuO (JCPDS 44-0706), $NiFe_2O_4$ (JCPDS No. 100325), and $ZnFe_2O_4$ (JCPDS No. 22-102) (Fig. 1). Significant diffraction peaks were indexed to the (220), (311), (400), (422), (511), and (440) crystal planes and all indicate a cubic spinel type of structure. Lack of secondary phases and impurity peaks denotes that the synthesized ferrites have high phase purity. The difference in peak intensities and minor broadening of peaks within a sample was indicative of the different size and extent of crystallinity in the samples that can be attributed to the ionic radii and combustion trends of the metal nitrates [17]. The high surface-to-volume ratio, as well as the better interface charge transport feature of these nanosized crystallites, make them good candidates in photocatalytic applications.

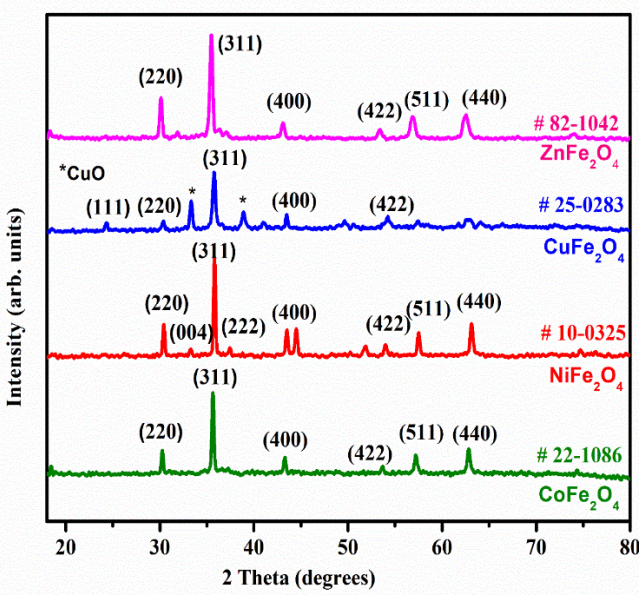

Fig. 1. PXRD of the synthesized ferrites.

Surface Morphology Analysis (SEM)

$CoFe_2O_4$, $NiFe_2O_4$, $CuFe_2O_4$ and $ZnFe_2O_4$ nanoparticles prepared by hybridization were characterized in terms of surface morphology by Scanning Electron Microscope (SEM). SEM micrographs showed that all ferrite samples had a very porous, loosely agglomerated morphology, which is common to substances synthesized by the solution

combustion technique. The high speed of the exothermic redox reaction on combustion forms a great deal of gases (*e.g.*, CO_2, N_2, and H_2O vapor), and this causes the foaming and porous character in the final product.

The $CoFe_2O_4$ nanoparticle exhibited an almost spherical shape of moderate agglomeration, having a spongy structure, which is found to be advantageous in the photocatalytic process because the surface area and contact points increase. The $CuFe_2O_4$ particles were found to be irregular in structure and have huge zones of pores, which may be attributed to the volatile nature of the copper precursors affecting the dynamics of combustion. Where $NiFe_2O_4$ was used, the particles are of a slightly finer and evenly dispersed nature, and there was little hard agglomeration; thus, the combustion was much controlled. $ZnFe_2O_4$ revealed a flake or platelet structure with porous networks that are interconnected, possibly coming about because of less exothermicity in combustion due to the lower enthalpy of zinc nitrate decomposition [18]. The SEM findings as a whole proved that the samples in question had a very porous microstructure, which is expected to facilitate the process of dye adsorption and, consequently, its photodegradation. Such a morphology leads to improved absorption of light, more interaction between the dye and catalyst, and more production of reactive oxygen species (ROS) through photocatalysis. To supplement the SEM examination, EDS (Energy Dispersive X-ray Spectroscopy) was carried out, demonstrating the elemental presence of Fe, O, and respective transition metals (Co, Cu, Ni, Zn) in the entire samples, and no traces of impurity were recorded, which points to the high purity of the synthesized ferrites.

HRTEM

The $CoFe_2O_4$, $NiFe_2O_4$, $CuFe_2O_4$ and $ZnFe_2O_4$ nanostructures are identified by HR-TEM, and the captured HR-TEM images are illustrated in Fig. 3 and 3a) reveals that the prepared $ZnFe_2O_4$ nanomaterials have spherical morphology, and Fig. 3b) shows the lattice fringes value is 0.253 nm, which corresponds to the (311) plane with an inset fig SAED pattern. Figure 3c depicts $CuFe_2O_4$, which displays the irregular morphology and Fig. 3d illustrates that the lattice fringes value is 0.282 nm of d-spacing with respect to its SAED pattern corresponding to the (311) plane. The agglomerated morphology obtained for $NiFe_2O_4$ (Fig. 3e), with a lattice fringe, is shown in Fig. 3f of d-spacing 0.251 nm, corresponding to its (311) plane. Figure 3g depicts $CoFe_2O_4$, which displays an irregular agglomerated morphology, and Fig. 3h illustrates that the lattice fringes value is 0.253 nm of d-spacing with respect to its SAED pattern corresponding to the (311) plane.

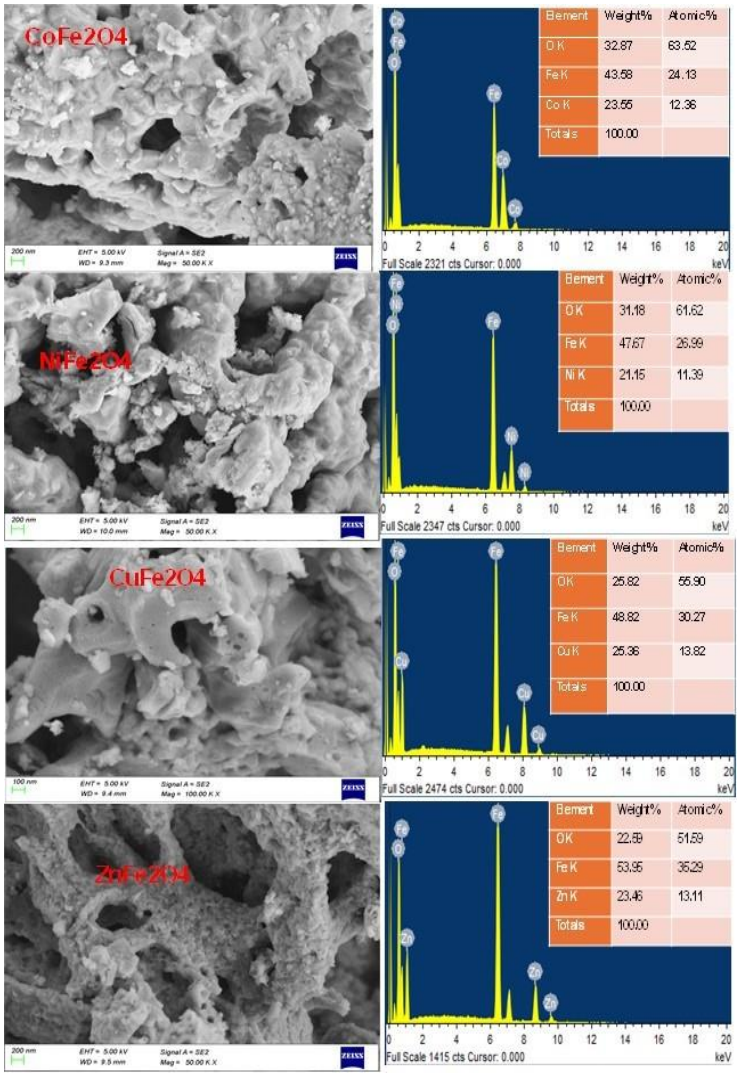

Fig. 2. (a-d) SEM images of $CoFe_2O_4$, $NiFe_2O_4$, $CuFe_2O_4$ and $ZnFe_2O_4$ and (e-h) EDX of $CoFe_2O_4$, $NiFe_2O_4$, $CuFe_2O_4$ and $ZnFe_2O_4$.

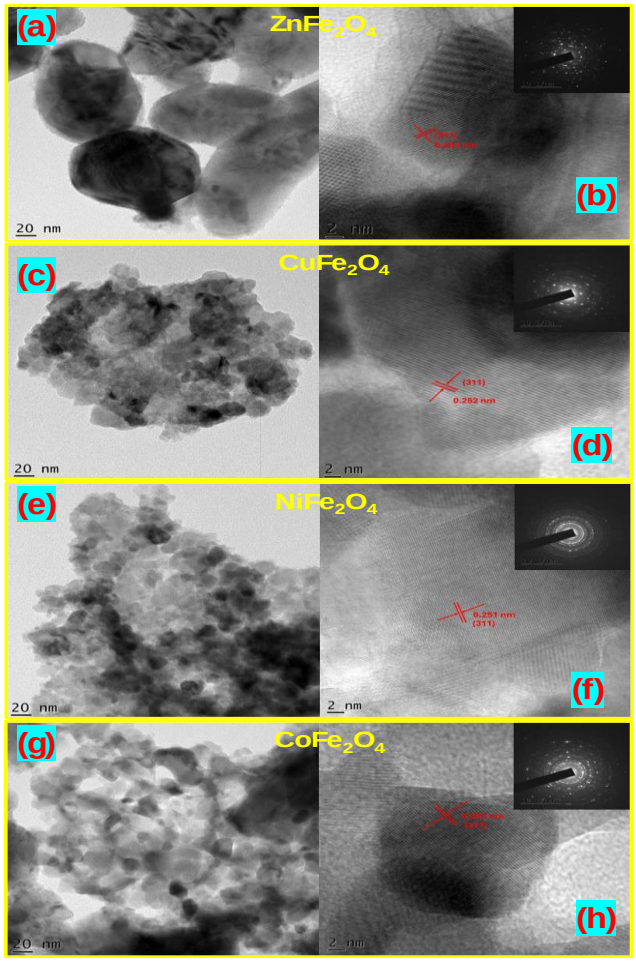

Fig. 3. (a,c,e,g) HRTEM images of $ZnFe_2O_4$, $CuFe_2O_4$, $NiFe_2O_4$ and $CoFe_2O_4$ (b,d,f,h) lattice fringes of $ZnFe_2O_4$, $CuFe_2O_4$, $NiFe_2O_4$ and $CoFe_2O_4$ with inset SAED of $ZnFe_2O_4$, $CuFe_2O_4$, $NiFe_2O_4$ and $CoFe_2O_4$.

UV-Visible Diffuse Reflectance Spectroscopy (UV-DRS)

UV-Vis Diffuse reflectance spectroscopy (Anderson) was used to find out the optical properties of the synthesized nanoparticles in the wavelength range between 200 to 800 nm in terms of band gap energies of $CoFe_2O_4$, $NiFe_2O_4$, $CuFe_2O_4$ and $ZnFe_2O_4$. All samples showed deep absorption in the visible part, which proves their ability to be used as visible-light-driven photocatalysts. The reflectance data were calculated as the absorption edge of each ferrite and converted by means of the Kubelka Munk functional: $F(R) = (1-R)^2/2R$, where R is the reflectance. Tauc plots were used in the production of optical band gap (E_g) values which were estimated by extrapolating the linear component of $(F(R)\ h\nu)^n$ towards $h\nu$, where n = 2 in direct band gap semiconductors, and n = 1/2 in indirect band gap semiconductors [19].

Band Gap Estimated for $CoFe_2O_4$, $NiFe_2O_4$, $CuFe_2O_4$ and $ZnFe_2O_4$ is in the range of 1.6-2.4eV (Fig. 4a and b). It is also seen that the ferrites have small differences in band gap energies that are attributed to the different electronic structure and the crystal field effect that the transition metal ions (Co^{2+}, Cu^{2+}, Ni^{2+} and Zn^{2+}) create in the spinel structure. $ZnFe_2O_4$ had the broadest band gap and $CuFe_2O_4$, the narrowest, to suit better absorption under the visible light. These band gap values signify that all the synthesized ferrites show a good absorption property of visible light and can separate the photogenerated charge carriers, and are useful in solar-driven or visible-light-assisted photocatalytic use to degrade dyes.

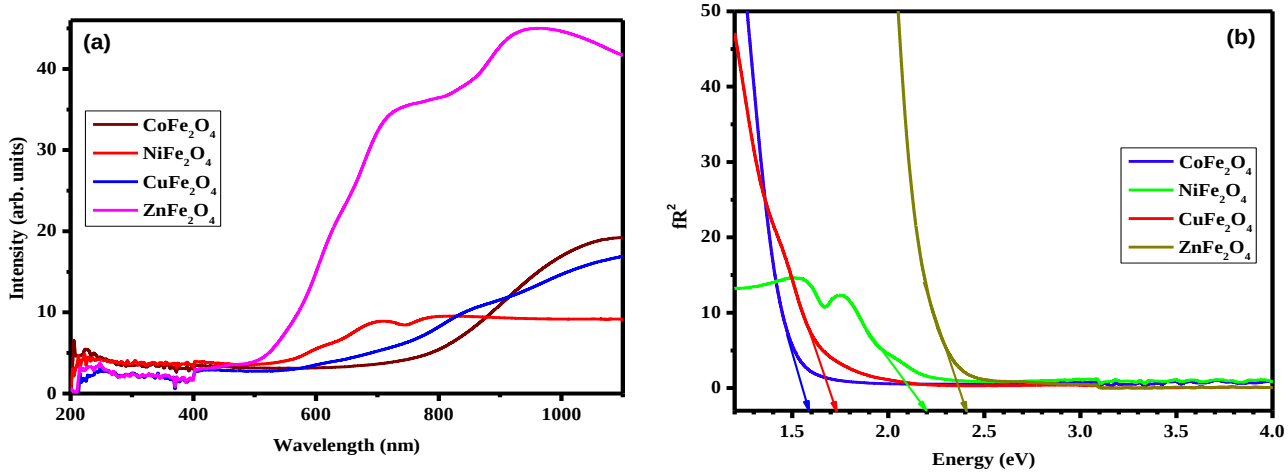

Fig. 4. a) UV-DRS studies of synthesized ferrites and b) the respective band gap.

Photoluminescence Studies

The photoluminescence (PL) studies are mainly characterized by the cationic distribution, metal-oxygen coordination and the intrinsic defect states. The transition metal ferrites typically exhibit the blue-green emissions due to oxygen vacancy and the Fe^{3+}-O charge transfer transitions, reflecting their partially inverted structure and high defect density. The synthesized ferrites PL studies are shown in Fig. 5 which indicates that $ZnFe_2O_4$ shows the weakest response among other ferrites, and $CuFe_2O_4$ shows the strongest peak in the PL. The other $CoFe_2O_4$ and $NiFe_2O_4$ show almost a similar type of emission peaks. The lowest peak intensity $ZnFe_2O_4$ thus confirms that the reduced radiative recombination of photogenerated electron-hole pairs, which facilitates more effective interaction of electrons and holes with adsorbed substrates, leads to the highest photocatalytic degradation.

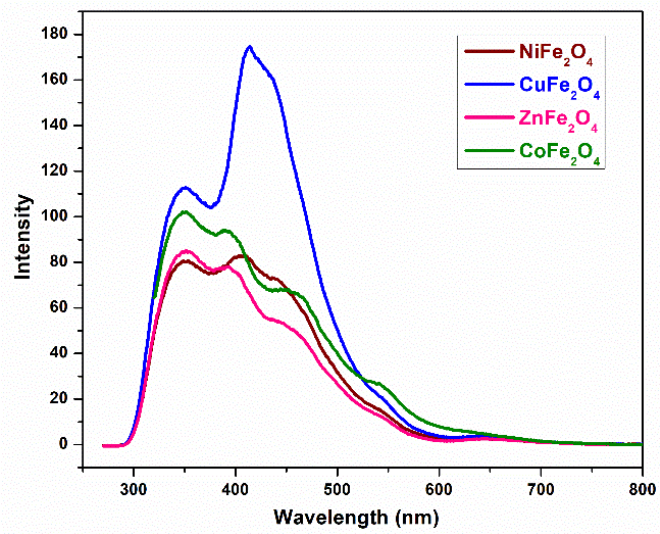

Fig. 5. PL studies of synthesized ferrites.

Photocatalytic Studies

A 125 W medium-pressure mercury vapour lamp was employed as the light source for the photocatalytic studies, which were carried out at room temperature in a circular glass reactor with a 176.6 cm^2 area.

MFe_2O_4 (M= Co, Ni, Cu and Zn) nanoparticles (NPs) were examined in order to examine the photocatalytic performance for the breakdown of Allura dye, an example of a pollutant. 50 mg of photocatalyst and 100 ml of ARD with a 10 ppm concentration were placed in a circular glass reactor. The sample and the light source should be separated by 25 cm. As the dye solution stirred in the dark, the catalyst reached equilibrium between adsorption and desorption. After the liquid solution supernatant is periodically collected. The dispersed amount of catalyst were separated using a centrifuge, and the corresponding concentration of dye that remained after a specified amount of time was measured using a UV-Visible spectrophotometer. Figures 6a-d displays the absorbance spectra of ARD degradation utilizing synthesized transition metal ferrites at intervals of 15 min. It unequivocally demonstrates that the maximum peak intensity at 505 nm drops as the time interval increases, confirming the degradation of ARD. Using $CoFe_2O_4$, $NiFe_2O_4$, $CuFe_2O_4$ and $ZnFe_2O_4$ as catalysts, the percentage degradation of ARD was determined to be 92.7%, 91.3%, 95.3%, and 97.5%, respectively (Fig. 6f and Table 1).

Table 1. Kinetic Studies under Visible Light MFe_2O_4 (M = Co, Ni, Cu, Zn) Photo Catalyst

Sl No	Catalyst	%Degradation	Rate (K)
1	$CoFe_2O_4$	92.7	0.02811
2	$NiFe_2O_4$	95.3	0.03889
3	$CuFe_2O_4$	91.3	0.02479
4	$ZnFe_2O_4$	97.5	0.03926

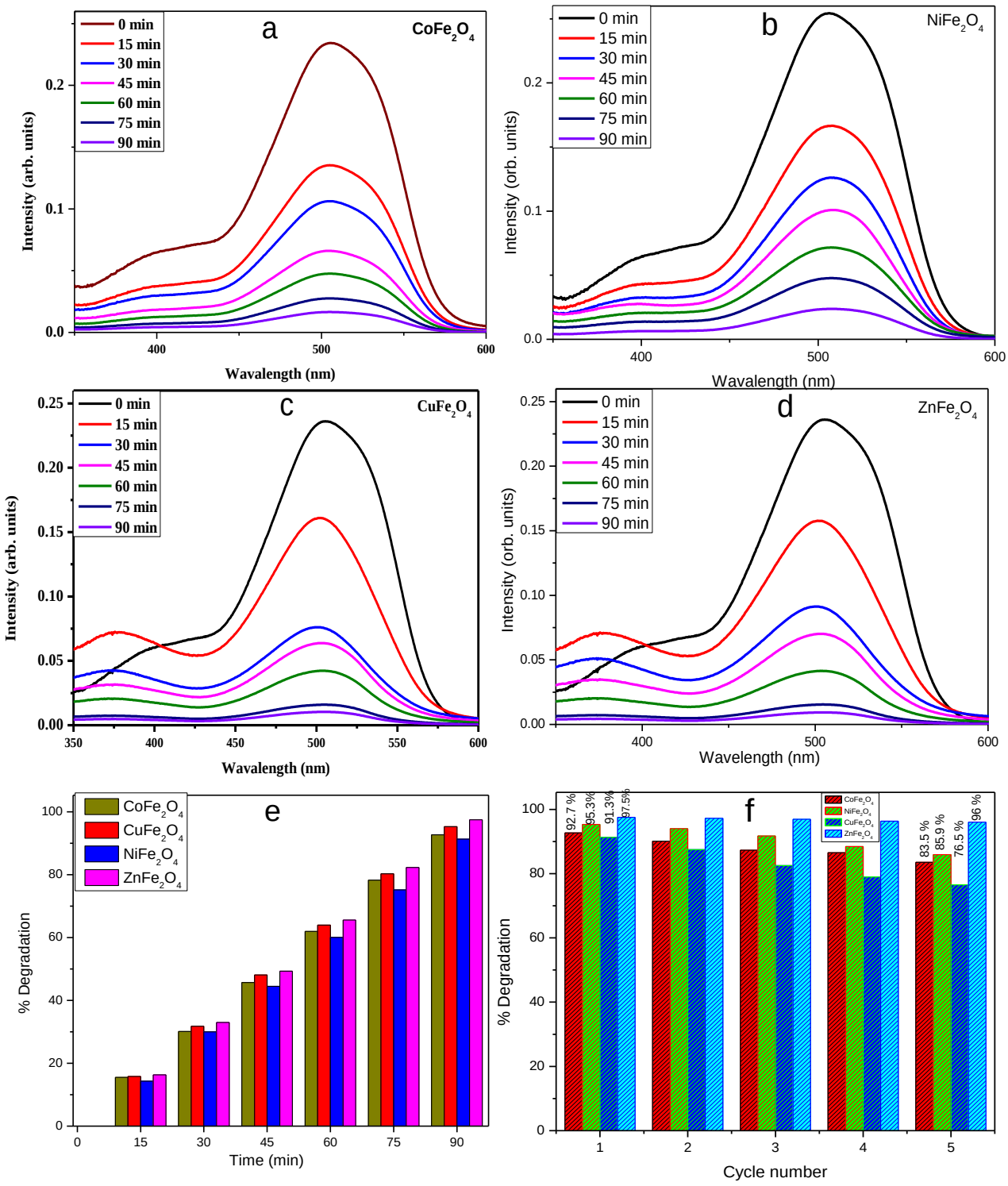

Fig. 6. Absorbance graph of allura red dye with a) $CoFe_2O_4$ catalyst, b) $NiFe_2O_4$ catalyst, c) $CuFe_2O_4$ catalyst, d) $ZnFe_2O_4$ catalyst, e) %Degradation of ARD with time, and f) Reusability of catalysts.

Mineralization of the contaminant was analyzed by measuring the percentage of residual total organic carbon (TOC) content after 90 min of reaction. Conducting the reaction in the absence of a photocatalyst results in approximately a 3% TOC removal; however, using synthesized ferrites as a support promotes TOC removal. By employing $CoFe_2O_4$, $NiFe_2O_4$, $CuFe_2O_4$ and $ZnFe_2O_4$ achieves a TOC removal of 31%, 22%, 43% and 52% respectively (Fig. 7).

Mechanism. When visible light strikes the catalyst transition metal ferrite in the allura red dye solution, it absorbs the light and produces electron-hole pairs. In addition to H_2O reacting with holes in the valence band to make •OH radicals, the generated electrons in the conduction band also react with the dissolved oxygen in the dye solution to form a superoxide anion (O^{2-}). Degradation happens when allura red molecules interact with the produced superoxide anions (O^2) and OH radicals, and is shown in Fig. 8. The greatest deterioration of ARD is shown in zinc ferrites, which may be caused by the optimum particle size, the morphology of ferrite and the ideal energy band gap of 2.4 eV [20].

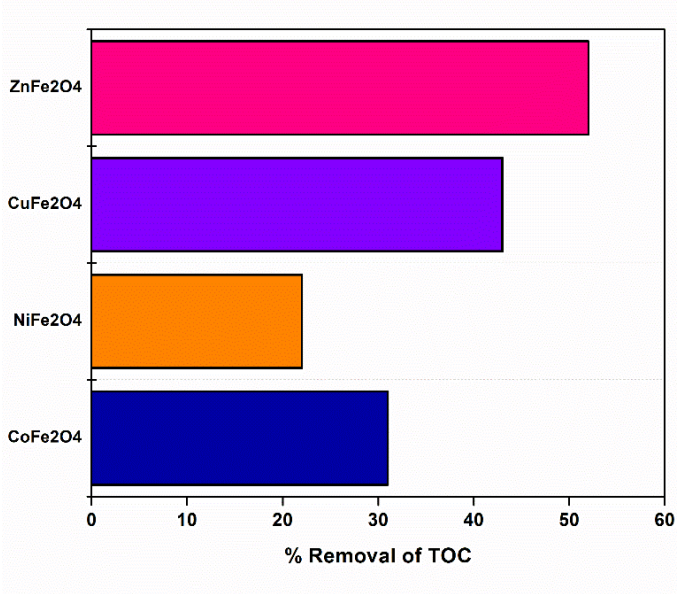

Fig. 7. %Degradation of TOC.

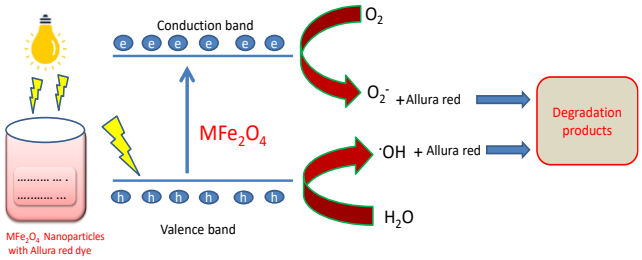

Fig. 8. Possible radical mechanism of dye degradation.

Reusability. Additionally, the reusability test was conducted for all the ferrites, using a dosage of 50 mg of photo catalysts, a reaction time of 90 min, and an allura red dye concentration of 10 ppm. Five consecutive runs were conducted in order to determine the stability and decreasing efficiency loss following each run, and are shown in Fig. 6f. The %deterioration for five cycles, even after five passes, the declining efficiency hardly changed. $CoFe_2O_4$, $NiFe_2O_4$, $CuFe_2O_4$ and $ZnFe_2O_4$ catalysts, the percentage degradation decreased from 92.7%, 91.3%, 95.3%, and 97.5% to 83.5%, 85.9%, 76.5% and 96 % respectively for the 1st to 5th cycle. This could be because remnants of the catalyst were lost during the subsequent cycles of filtration. It was demonstrated that a $ZnFe_2O_4$ photocatalyst can degrade ARD effectively than other ferrites and with a high potential for reuse.

ELECTROCHEMICAL STUDIES

Cyclic Voltammetry (CV)

The oxidation and reduction processes of synthesized ferrites were studied by cyclic voltammetry (CV) method using a conventional three-electrode cell, stainless steel, using ferrite-impregnated glassy carbon electrode (GCE) as the working electrode, a platinum wire as the counter electrode and Ag/AgCl as the reference electrode in 0.1 M KCl or phosphate-buffered saline (PBS, pH 7.0) solution.

These CV tests were quasi-reversible redox and the anodic/cathodic peaks relating to the redox change of Fe^{3+}/Fe^{2+} and M^{2+}/M^{3+} (where M = Co, Cu, Ni and Zn). $NiFe_2O_4$ and $CoFe_2O_4$ had the greatest peak current and the least peak separation, hence they have increased the electrochemical activity and pre-eminent kinetics of electron transfer (Fig. 9a).

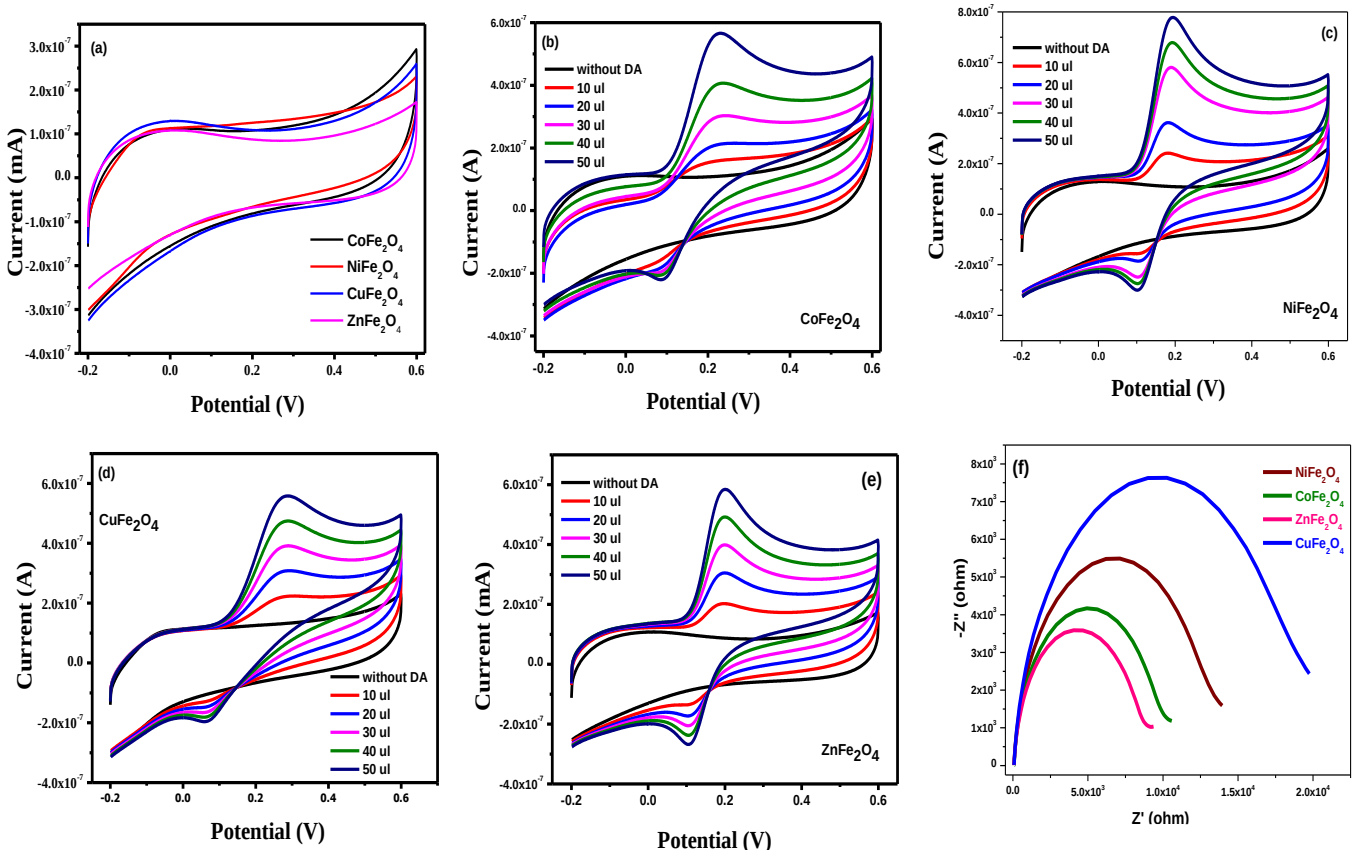

Fig. 9. a) CV studies of synthesized ferrites, (b-e) sensor studies of $CoFe_2O_4$, $NiFe_2O_4$, $CuFe_2O_4$ and $ZnFe_2O_4$, (f) Nyquist plots of $CoFe_2O_4$, $NiFe_2O_4$, $CuFe_2O_4$ and $ZnFe_2O_4$.

Electrochemical Impedance Spectroscopy (EIS)

The frequency range of EIS done was between 0.01 Hz and 100 kHz at open-circuit potential with the AC signal amplitude of 5 mV (Fig. 9f). Characteristic Nyquist plots were recognizable, having a normal semicircular area at high frequencies and a straight area at low frequencies. The value of charge transfer resistance (Rct) was obtained by measuring the diameter of the semicircle. The Rct resistance values extracted from the curves were $8.74 \times 10^4\ \Omega$ for $ZnFe_2O_4$ electrode, $CoFe_2O_4$ electrode ($9.97 \times 10^4\ \Omega$), $NiFe_2O_4$ electrode ($13.34 \times 10^4\ \Omega$) and $CuFe_2O_4$ electrode ($18.65 \times 10^4\ \Omega$) which reflects that $ZnFe_2O_4$ electrode has a good conductivity [21,22].

Electrochemical Sensing Performance

Dopamine is a vital neurotransmitter whose abnormal concentrations are strongly associated with major neurological and psychiatric disorders. Sensitive and selective detection of dopamine is essential for clinical diagnosis, therapeutic monitoring, neuroscience research, and drug development. Therefore, developing reliable electrochemical sensors for dopamine is of significant biomedical and analytical importance [23,24].

The modified electrodes were evaluated for their sensor response toward model analytes like dopamine (DA), using CV studies (Fig. 9b-e). Among the ferrites, $NiFe_2O_4$-modified GCE displayed superior sensitivity and better selectivity due to fast charge transfer and higher electroactive surface area.

These results confirm the potential of transition metal ferrites especially $NiFe_2O_4$ and $CoFe_2O_4$ as promising electrochemical materials for sensor applications due to their optimal band structure, nanostructured morphology, and good redox activity.

CONCLUSION

This work has illustrated the synthesis of nanoparticles $CoFe_2O_4$, $CuFe_2O_4$, $NiFe_2O_4$, and $ZnFe_2O_4$ to be successfully synthesized via the solution combustion method by obtaining porous nanostructured material that is suitable for photocatalytic applications due to the high surface area to volume ratio. The scanning electron microscopy analysis revealed the high porosity of the morphology associated with the synthesis of ferrites using combustion. The UV Visible spectrophotometer shows the band gap range from 1.6-2.4 eV. The photocatalytic activity of all the samples was good under the action undervisible light. The degradation results shown by $ZnFe_2O_4$ of 97.5% which is better than $CoFe_2O_4$ (92.7%), $NiFe_2O_4$ (95.3%) and $CuFe_2O_4$ (91.3%). On the whole, the research proves that the transition metal ferrites will be good candidates to degrade effectively and in an eco-friendly manner the harmful dyes such as Allura Red, which points to solutions to treat wastewater chemicals and conserve the environment. Further synthesized ferrites were showing the best results in sensing dopamine, in which $NiFe_2O_4$ shows enhanced sensing activity than other ferrites. Hence, these results show multiple applications of the ferrites.

REFERENCES

[1] Singh, D.; Sharma, P., Visible-light-driven degradation of azo dyes using ferrite-based heterostructures: A comparative study. *Environ. Nanotechnol. Monit. Manage.* **2024**, *22*, 100789. DOI: 10.1016/j.enmm.2024.100789.

[2] Gurushantha, K.; Keshavamurthy, K.; Shashidhar, S; Meena, S., Facile Synthesis of Spinel Zinc Aluminate Using Biofuel for Effective Photocatalytic Dye Degradation and Electrochemical Sensor Studies. *J. Mines Met. Fuels.* **2023**, *71*(11). DOI: 10.18311/jmmf/2023/36051.

[3] Mohammed, R. H.; Jassim, L. S.; Shihab, M. H., Photocatalytic degradation of Allura Red dye using CuO nanosheets prepared by hydrothermal method. *Egypt. J. Chem.* **2021**, *64*(5), 2461-2468. DOI: 10.21608/ejchem.2021.60267.3084.

[4] Marín-González, A.; Velo-Gala, I.; Rico-Cerda, J.; Fernández-González, C., Allura Red degradation using Co/Al–PILC in a heterogeneous Fenton-like process: Mechanism and mineralization efficiency. *Chem. Eng. J. Adv.* **2024**, *17*, 100449. DOI: 10.1016/j.ceja.2024.100449.

[5] Roopashree, B. N.; Gurushantha, K.; Nagaraju, K.; Meena, S., Recent Review On S-Scheme Photocatalysis, *Water Air Soil Pollut.* **2024**, *235*(570), 2024, https://doi.org/10.1007/s11270-024-07376-y.

[6] Kumar, S.; Chauhan, M.; Saini, R.; Kumar, A., Highly efficient visible light driven catalytic activity of $ZnFe_2O_4$ for degradation of reactive violet 5R dye: A mechanistic insight. *Catalysts.* **2023**, *13*(7), 1061. DOI: 10.3390/catal13071061.

[7] Kumar, M.; Sharma, R.; Satsangi, V. R., Visible-light responsive $CoFe_2O_4$@MoS_2 and $Co_{0.5}Ni_{0.5}Fe_2O_4$@MoS_2 nanocomposites for enhanced photocatalytic degradation of organic pollutants. *Eur. Phys. J. Plus.* **2024**, *139*, 5584. DOI: 10.1140/epjp/s13360-024-05584-1.

[8] Yadav, A. K.; Kumar, A., Tailoring the catalytic performance of $Mg_xZn_{1-x}Fe_2O_4$ spinel nanoparticles: An efficient route for dye degradation under visible light. *Int. J. Photoenergy.* **2023**, Article ID 9780955. DOI: 10.1155/2023/9780955.

[9] Sharma, K.; Guleria, A.; Chauhan, P., Sol-gel synthesized α-Fe_2O_3, $NiFe_2O_4$ and $ZnFe_2O_4$: Characterization and their comparative photocatalytic performance for azo dye degradation. *Int. J. Photoenergy.* ***2023***, Article ID 3257914. DOI: 10.1155/2023/3257914.

[10] Ameen, M.; Khan, M. S., Photocatalytic efficiency of $CoFe_2O_4$/TiO_2 nanocomposites under UV light: Synthesis, characterization and dye degradation studies. *J. Mater. Sci.: Mater. Electron.* **2022**, *33*, 15783-15795. DOI: 10.1007/s10854-022-08227-5.

[11] Kumar, A.; Jha, P. K., Advances in ferrite-based nanomaterials for environmental remediation: A review. *J. Environ. Chem. Eng.* **2023**, *11*(1), 109837. DOI: 10.1016/j.jece.2022.109837.

[12] Singh, J.; Soni, R. K., Transition metal ferrite nanoparticles for visible light photocatalysis: A

comprehensive review. *Mater. Sci*. **2022**, *1066*, 113-138. DOI: 10.4028/www.scientific.net/ MSF.1066.113.

[13] Zhu, Q.; Wang, W.; Zhang, Y.; Xu, H., A novel $CuFe_2O_4/TiO_2$ heterojunction nanocomposite for enhanced visible-light-driven degradation of organic pollutants. *RSC Adv*. **2024**, *14*(18), 4323-4332. DOI: 10.1039/D4RA04334K.

[14] Pan, Y.; Li, X.; Liu, Y.; Wu, D., Magnetic and photocatalytic properties of $NiFe_2O_4$ nanoparticles synthesized by a combustion method. *Inorganics*. **2022**, *10*(6), 143. DOI: 10.3390/inorganics10060143.

[15] Al-Hetlani, E.; Al-Kandari, H., Efficient degradation of Allura Red using $ZnFe_2O_4/TiO_2$ nanocomposite under visible light. *Catalysts*. **2021**, *11*(12), 1543. DOI: 10.3390/catal11121543.

[16] Gujjaramma, H.; Gurushantha, K.; Meena, Green synthesis of Eu-doped yttria-stabilized zirconia, characterization, and its applications as photocatalyst and antibacterial activities. *Ionics*. **2025**, DOI: 10.1007/ s11581-025-06275-4.

[17] Shashidhar, S.; Vidyavati, A.; Shastry, K.; Gurushantha, K.; Brungesh, V.; Meena, S.; Anantharaju, K. S.; Raghu, G. K., Ceramic manganese ferrite: synthesis, characterisation and its applications as photocatalyst and electrochemical studies. *Rasayan J. Chem.,* **2025**, *18*(1), 1-6. DOI: 10.31788/RJC.2025.1819075.

[18] Roopashree, B. N.; Gurushantha, K.; Nagaraju Kottam, Ashly, P. C.; Meena, S.; Keshavamurthy, K.; Raghu, G. K., Atthasit Tawai, S-scheme ZnO/g-C_3N_5 visible light active photocatalyst for Rhodamine B dye degradation and Hg sensing applications. *Appl. Sci. Eng. Prog.* **2025**, *18*(4), 7783. http://dx.doi.org/10.14416/ j.asep.2025.06.001

[19] Khan, A.; Ahmad, S., Green synthesis of $NiFe_2O_4$ nanoparticles using plant extract for photocatalytic degradation of Congo red dye under sunlight. *Mater. Today Proc.* **2022**, *61*, 1145-1150. DOI: 10.1016/j.matpr.2022.06.051.

[20] Swamy, S.; Gurushantha, K.; Meena, S.; Shashidhar, S.; Srinatha, N.; Anantharaju, K. S.; Aruna Kumar, D. B.; Soumya, C.; Deepa, D.; Nivedita, R. D., Clove Oil mediated combustion method synthesised Dy stabilized Lanthanum Ferrite its application as Photocatalyst and Antibacterial agent. *Desalination water treat.* **2024**, *320*, 100785. DOI: 10.1016/j.dwt.2024.100785.

[21] Pournemati, Kh.; Habibi-Yangjeh, A., Recent insights on Z-scheme and S-scheme photocatalysts for nitrogen conversion to ammonia: A review, *Mater. Today Sustain.***,** *Mater. Today Sustain.,* **2024**, *28*, 101043, ISSN 2589-2347, https://doi.org/10.1016/ j.mtsust.2024.101043.

[22] Seifikar, F.; Habibi-Yangjeh, A.; Jahed-Jaafargolikhanlo, M., A critical review on emerging photothermal-photocatalytic materials composed of g-C3N4 for energy production and environmental remediation, *J. Environ. Chem. Eng.,* **2025**, *13*(2) 115812, ISSN 2213-3437, https://doi.org/10.1016/ j.jece.2025.115812.

[23] Habibi-Yangjeh, A.; Pournemati, Kh., *Crit. Rev. Environ. Sci. Technol.*, **2024**, 54, 4, 290-320(31).

[24] Seifikar, F.; Habibi-Yangjeh, A., Floating photocatalysts as promising materials for environmental detoxification and energy production: A review. *Chemosphere*. **2024**, *355*, 141686. DOI: 10.1016/j.chemosphere.2024.141686.